LINE FORMATION IN SPHERICAL MEDIA WITH PARTIAL FREQUENCY REDISTRIBUTION

II. *Expanding Media with Redistribution Function* R_{I}.

A. PERAIAH
Indian Institute of Astrophysics, Bangalore, India

(Received 12 January, 1979)

Abstract. Lines formed in a differentially expanding atmosphere have been calculated by using the angle averaged redistribution function R_{I} (Hummer, 1962). We have compared these lines, in a few cases, with those formed by complete redistribution in the observer's frame of reference. We have considered an atmosphere whose ratios of inner to outer radii are 2 and 10, and it is assumed that the gas in the atmosphere is expanding uniformly with a maximum velocity of 3 mean thermal units. We have presented lines formed in spherical symmetry and those obtained by integrating over the apparent disc. Three types of physical situations are considered with a 2-level atom with non-LTE approximation (1) $\varepsilon = 10^{-4}$, $\beta = 10^{-4}$, (2) $\varepsilon = 10^{-4}$, $\beta = 0$ and (3) $\varepsilon = \beta = 0$, where ε is the probability per scatter that a photon is destroyed by collisional de-excitation, and β is the ratio Kc/Kl of absorption in the continuum per unit frequency interval to that in the line centre.

It is found that there are noticeable differences between the profiles formed by partial redistribution (PRD) and complete redistribution (CRD). The profiles integrated over the stellar disc from the first type of the media are box type with flat top, which are similar to those observed in WC stars and those from the second type of media show emission peaks on red and blue sides with emission on the red side larger than the one on the blue side. The profiles from the third type of media with pure scattering, show some emission on the red side and deep absorption on the blue side. Large geometrical extensions of the atmosphere and higher gas velocities seem to enhance these two effects.

1. Introduction

The observed spectral lines of many stars show evidence that the matter in their outer layers is moving outwards among which the Wolf-Rayet stars are well-known (see, for example, Bappu, 1973; Kuhi, 1973). Theoretical calculations of lines from an expanding atmosphere are of considerable difficulty. McCrea and Mitra (1936) and Chandrasekhar (1945) have made some of the earliest attempts at obtaining theoretical line profiles and more recently Abhyankar (1964) calculated lines in a plane parallel atmosphere with coherent scattering in the fluid frame. Subsequently, there were several attempts using plane parallel approximation and complete redistribution. Vardavas (1974, 1976), Cannon and Vardavas (1974), Mihalas *et al.* (1976) calculated lines using partial redistribution (PRD) in a differentially moving medium and made comparisons with those calculated by using complete redistribution (CRD). They have found differences between the calculations, which was confirmed by calculations of Peraiah (1978a, henceforth called Paper I, and 1978b). In Paper I, we have described a general method to calculate lines either in an expanding, or in a static, spherically symmetric media

Astrophysics and Space Science **63** (1979) 267–277. 0004–640X/79/0632–0267$01.65

with PRD, and lines formed in static media have been given in that paper to exhibit the differences between the lines formed in CRD and those formed in PRD. In this paper, we shall investigate the lines formed in differentially expanding spherically symmetric media with three different types of physical characteristics: (1) with continuous absorption and line emission ($\varepsilon = 10^{-4}$ and $\beta = 10^{-4}$), (2) without continuous absorption but with line emission ($\beta = 0$ and $\varepsilon = 10^{-4}$) and (3) a pure scattering medium ($\beta = 0$, and $\varepsilon = 0$). We shall also calculate the lines integrated over the visible disc so that these profiles can be compared directly with those observed.

The computational procedure and discussion of the results are presented in Section 2.

2. Computational Procedure and Discussion of the Results

The method of solution of the transfer problem described in Paper I has been employed to calculate the lines in differentially expanding media. The frequency $x\,(=(\nu - \nu_0)/\Delta\nu_D$ where $\Delta\nu_D$ is the Doppler width) becomes $x \to x \pm \mu\vartheta$ in the rest frame of the observer, where $\vartheta = \vartheta_{\text{gas}}/\vartheta_{\text{thermal}}$, the ratio of the gas velocity to the thermal velocity. $\mu = \cos\theta$ and $\pm$ signs refer to the oppositely directed beams of radiation. In a moving medium, we have to calculate all the four redistribution functions appearing in the scattering integral namely, $R(X + \mu\vartheta, X' + \mu\vartheta)$, $R(X - \mu\vartheta, X' - \mu\vartheta)$, $R(X + \mu\vartheta, X' - \mu\vartheta)$ and $R(X - \mu\vartheta, X' + \mu\vartheta)$ to evaluate the diffuse radiation field due to the moving matter (see Paper I). We have chosen 20 frequency points and 4 directions and employed the angle averaged redistribution function $R_{\text{I-A}}$ given by Hummer (1962) as

$$R_{\text{I-A}}(X, X') = \tfrac{1}{2}\,\text{erfc}(|\bar{x}|), \tag{1}$$

where

$$\text{erfc}\,(X) = \frac{2}{\sqrt{\pi}} \int_x^\infty e^{-t^2}\,\mathrm{d}t; \tag{2}$$

and the corresponding profile function in CRD is taken to be the Doppler profile given by

$$\phi(X) = \frac{1}{\delta\sqrt{\pi}}\, e^{-(X/\delta)^2}, \tag{3}$$

and δ is always put equal to 1. A uniformly expanding atmosphere (see Wehrse and Peraiah, 1978; Peraiah and Wehrse, 1978) has been considered with the velocity distribution $\vartheta(r)$ given by

$$\vartheta(r) = \vartheta(R_0) + \frac{\vartheta(R) - \vartheta(R_0)}{R - R_0}\, r, \tag{4}$$

where R_0 and R are the inner and outer radii of the atmosphere. We have calculated the profiles from two points of view: (1) in spherical symmetry which involves the direct solution of the radiative transfer equation and (2) the profiles integrated over

the visible disc which can be compared with the observations directly. As we have mentioned in the introduction, we shall consider the three types of media: namely, (1) $\varepsilon = \beta = 10^{-4}$; (2) $\varepsilon = 10^{-4}$, $\beta = 0$; (3) $\varepsilon = \beta = 0$.

In all the cases, the geometric extension is taken to be $B/A = 2$ and 10 where B and A are the outer and inner radii of the atmosphere, respectively. The optical depth is set to vary as r^{-2} and the total optical depth at line centre is taken to be 10^3 in all cases. We have set $\vartheta(R_0) = 0$ always and $V(R) = 0$, 1, 2 and 3 times the mean thermal velocity and let the velocity vary according to Equation (4). The medium has been divided into n shells, $n = 1$ being the outermost shell ($\tau = 0$) and $n = N$ being the inner most shell ($\tau = T$). The boundary condition for the first two cases are taken as

$$U_{N+1}^{-}(X, \mu, \tau = T) = U_1^{+}(X, \mu, \tau = 0) = 0; \tag{5}$$

and for the third case,

$$U_{N+1}^{-}(X, \mu, \tau = T) = B \quad \text{and} \quad U_1^{+}(X, \mu, \tau = 0) = 0,$$

where

$$U_n^{\pm} = 4\pi r_n^2 I(X, \mu, \tau);$$

$I(X, \mu, \tau)$ being the specific intensity. The Planck function B is kept constant throughout the medium in the calculation of the profiles in the first two cases and $B'_{n+1/2} = 4\pi r^2 B$ (see Equation (16) of Paper I). The maximum value of $V(R)$ that has been used in these calculations is 3 thermal units and this is because of the fact that when we take $V(R) > 3$, the solution of the radiative transfer shows signs of oscillations particularly when $\varepsilon = 0, \beta = 0$. This trouble can be avoided if we take more frequency points and angle points and a large enough band width. Moreover, test calculations, not presented here, show that when the total optical depth and the extension of the medium are increased, it is possible to consider large velocities.

In Figure 1 we have plotted the frequency independent source function for R_{I} (see Equation (27) of Paper I) against the shell number N, for velocities $V(R) = 0$, 1, 2 and 3 for the first type of the medium in which $\varepsilon = \beta = 10^{-4}$. The corresponding values for CRD are also presented for the sake of comparison and all these results are presented for the two geometrical extensions $B/A = 2$ and 10. One can immediately see that there are substantial differences between the source functions corresponding to R_{I} and CRD. The source functions for $B/A = 10$ lie considerably below those of $B/A = 2$. At $n = 1$ (near the surface of the atmosphere) the source functions for R_{I} are approximately the same whereas for CRD these are different and for larger geometrical extensions and high velocities these differences are even larger. The differences among the source functions for R_{I}, when high velocities are considered, are not too large for smaller values of B/A, but for large values of B/A these differences are substantial.

The emergent flux profiles (see Equation (28) of Paper I) in spherical symmetry corresponding to the source functions given in Figure 7 are plotted in Figure 2a for $V(R) = 0$, 1 and in Figure 2b for $V(R) = 2$ and 3 and the geometrical extension B/A

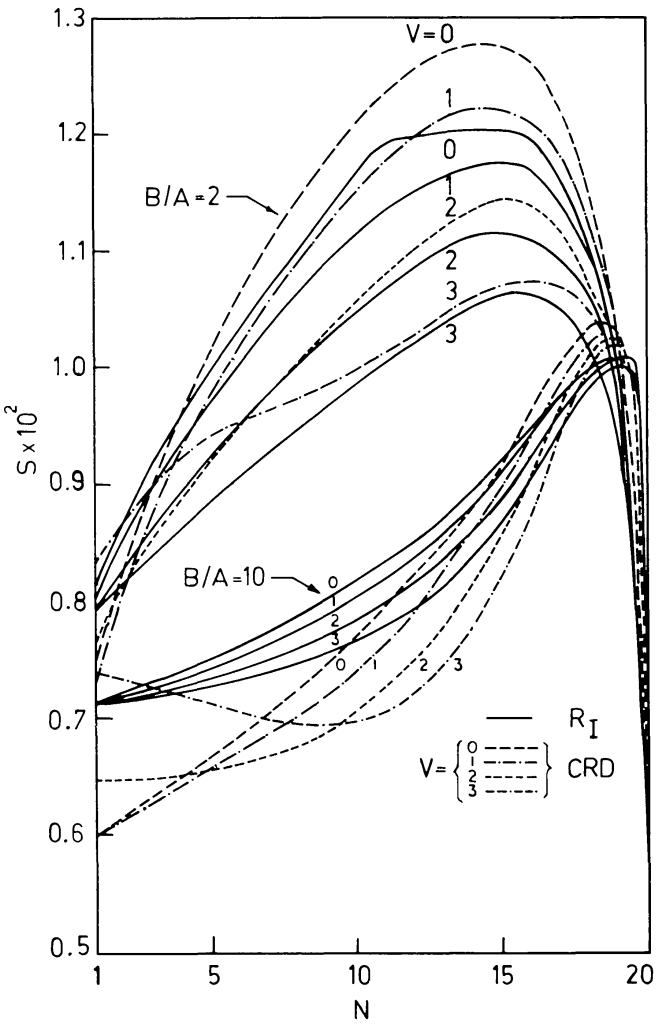

Fig. 1. Frequency-independent source functions of R_{I-A} and CRD are plotted against the shell number $B/A = 2$ and 10. $V(R) = 0$, 1, 2 and 3. $\epsilon = \beta = 10^{-4}$.

is taken to be 10. In a static case ($V(R) = 0$), the lines are symmetric about the centre and formed with strong emission in the wings with pronounced continuum. The shapes of the lines change in the differentially moving medium $V(R) > 0$, in that there is strong red emission and blue absorption together with a shift of the centre of the line towards the blue side approximately proportional to the velocity with which the gas is expanding. As the velocity increases the continuum disappears completely, one finds a P Cygni type profile (see Kunasz and Hummer, 1974; Vardavas, 1974). As we have seen in Paper I, there are large differences between the profiles calculated with PRD and CRD in a static medium, and now it is clear from the results presented here, that these differences continue to exist in a differentially moving media. For $V(R) = 1$, the red emission is quite large and as the velocity increases the height of the emission is reduced, but the line becomes broader.

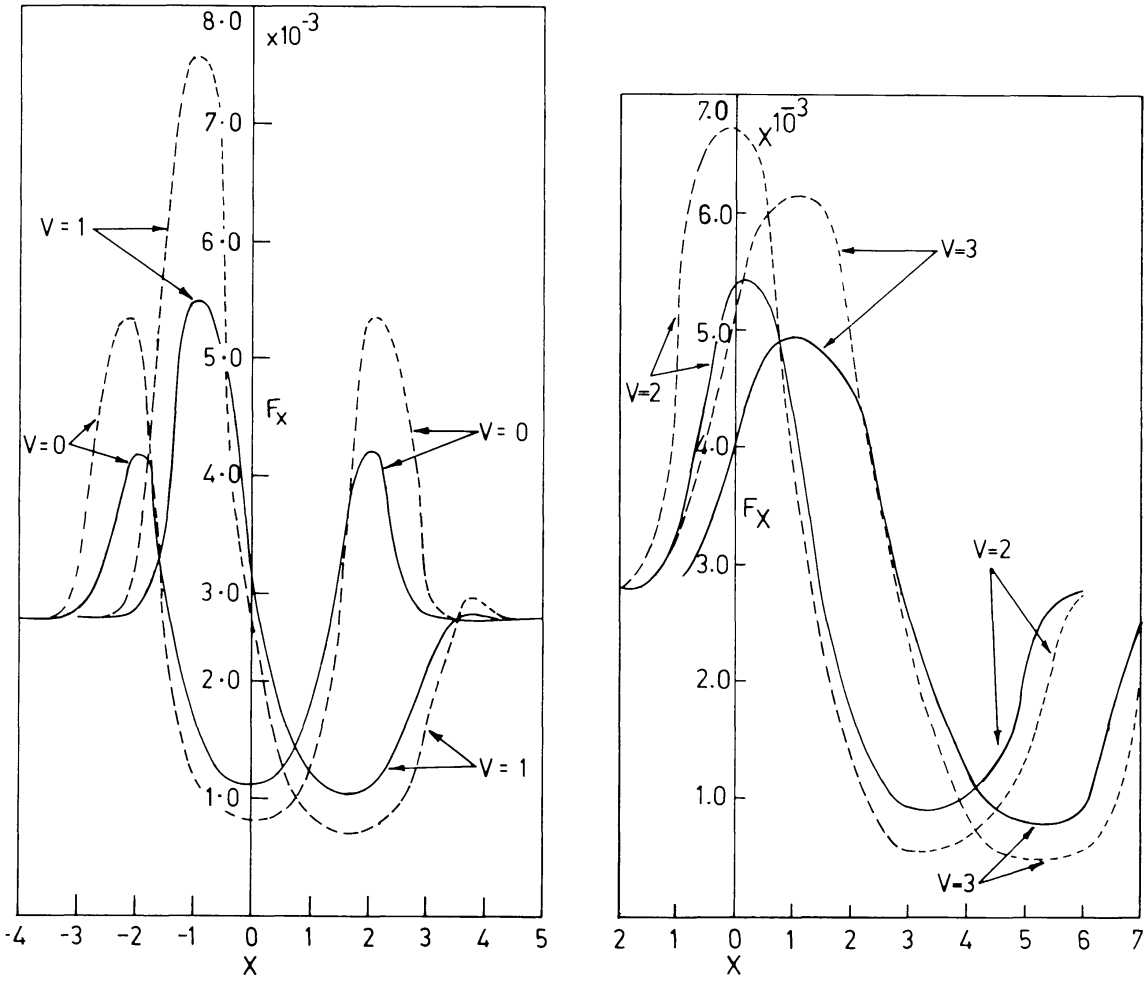

Fig. 2. Emergent flux profiles in spherical symmetry. (a) $B/A = 10$, $V(R) = 0, 1$, $\varepsilon = \beta = 10^{-4}$. ——, R_I; – – –, CRD. (b) $B/A = 10$, $V(R) = 2, 3$. $\varepsilon = \beta = 10^{-4}$. ——, R_I; – – – CRD.

In Figure 3a we have plotted the line profiles integrated over the visible disc (see, Mihalas, 1978; page 473, Figure 4-7) for $B/A = 2$ and 10, respectively. In Figure 3a the profiles corresponding to PRD and CRD are given for comparison and in Figure 3b only those corresponding to PRD are given for the sake of clarity of information. These profiles look considerably different from those presented in Figure 2 although some of the characteristics remain the same. The integrated profiles are asymmetric with red emission becoming broader with increasing velocities.

In a static atmosphere, a symmetric absorption profile with or without emission wings is formed from the material in the atmosphere directly between the star and the observer (refer again to Figure 14-7, page 473, Mihalas, 1978, let us call this region, A) and a symmetric emission profile from the regions of the atmosphere away from region A (we shall call these region B). When the gas in the atmosphere is moving

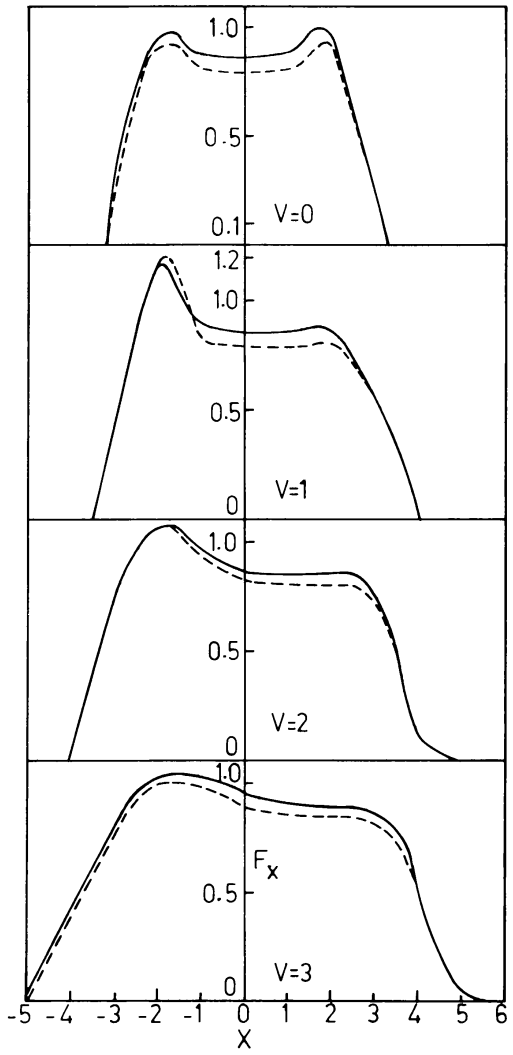

(a)

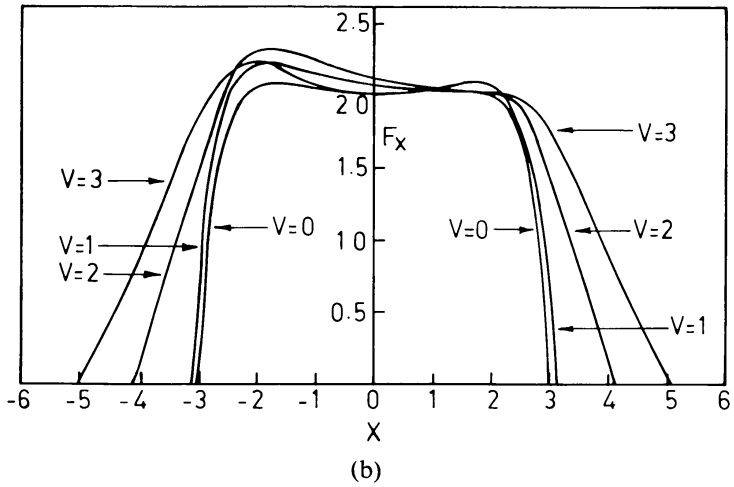

(b)

Fig. 3. (a) Integrated profiles for $B/A = 2$. $\varepsilon = \beta = 10^{-4}$. ——, R_I; – – –, CRD. Numbers on the ordinate are arbitrary. (b) Integrated profiles for $B/A = 10$ for R_I and $\varepsilon = \beta = 10^{-4}$.

radially outward, the radiation emitted by the gas in region A (which is moving directly towards the observer) is blue shifted and therefore, the absorption part of the line is shifted towards the blue side of the line centre. However, the radiation emerging from the gas moving away from the observer in region B is again scattered by that which is moving towards the observer before it emerges out of the atmosphere. This radiation reaches the observer together with that emitted by the gas moving towards the observer. Consequently, an asymmetry is introduced in the emission part of the line with a smaller shift than in the case of the absorption part and, therefore, the line appears to have enhanced emission on the red side. These profiles look similar to those of box-type with flat top given in Bappu (1973) and Kuhi (1973). Although the latter profiles look quite similar to those presented here, we cannot make a detailed comparison with those of former type as these profiles seem to extend over several decades of Doppler widths, whereas those presented here extend over approximately 10 Doppler widths corresponding to 3 thermal units of gas velocity.

In Figure 4, the frequency-independent source function corresponding to R_{I} is presented for $B/A = 2$ and 10 for case (2). The source functions shown here are different from those given in Paper I corresponding to the same ε and β, as these describe a medium with the optical depth varying as r^{-2} and the latter represent a homogeneous medium. The source functions are small at $N = 1$ and 20 because of the fact that no incident radiation has been applied on either boundary. For $B/A = 2$, they differ at $N = 1$ for various velocity distributions but for $B/A = 10$, they tend to be

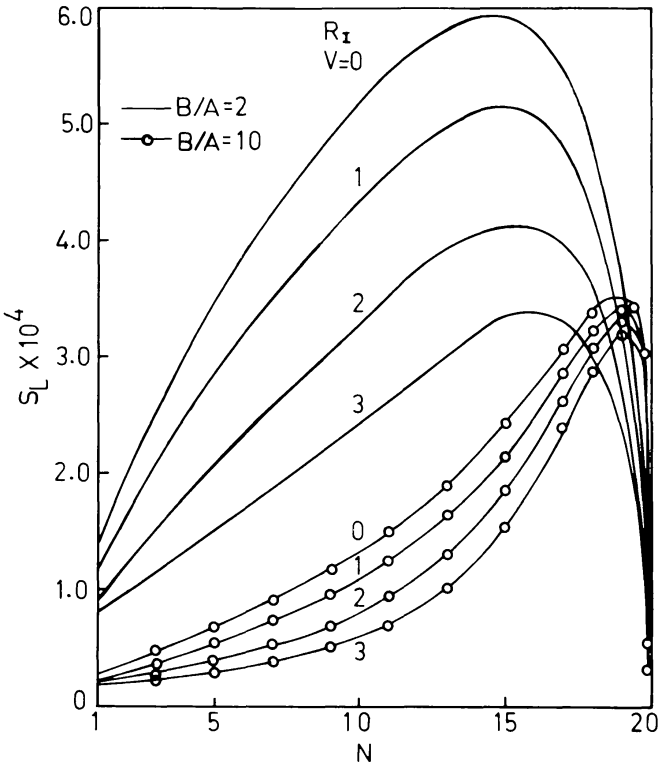

Fig. 4. Frequency-independent source functions for R_{I}. $B/A = 2$, 10. $\varepsilon = 10^{-4}$, $\beta = 0$.

equal although inside the medium, they differ substantially. They lie below one another for each $V(R)$ and the maximum of S shifts towards the inner boundary as the velocity increases because of the fact that the velocity increases from $V = 0$ at $N = 20$ to $V = V(R)$ at $N = 1$. The integrated profiles representing the source functions in Figure 4 are described in Figures 5a and 5b for $B/A = 2$ and 10 respectively. Unlike the profiles shown in Figure 3, we see here that there are two emission peaks one on each side of the centre of the line, the one on the red side being always larger than the

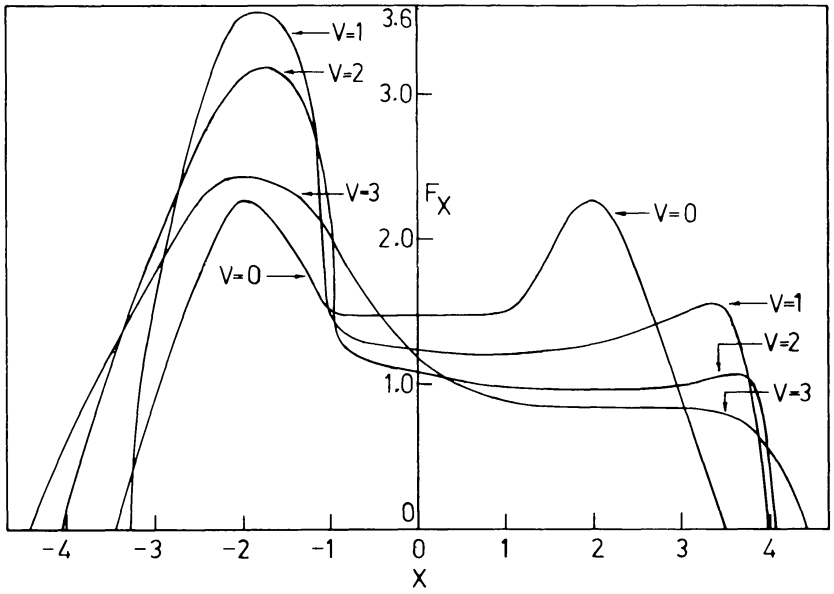

(a)

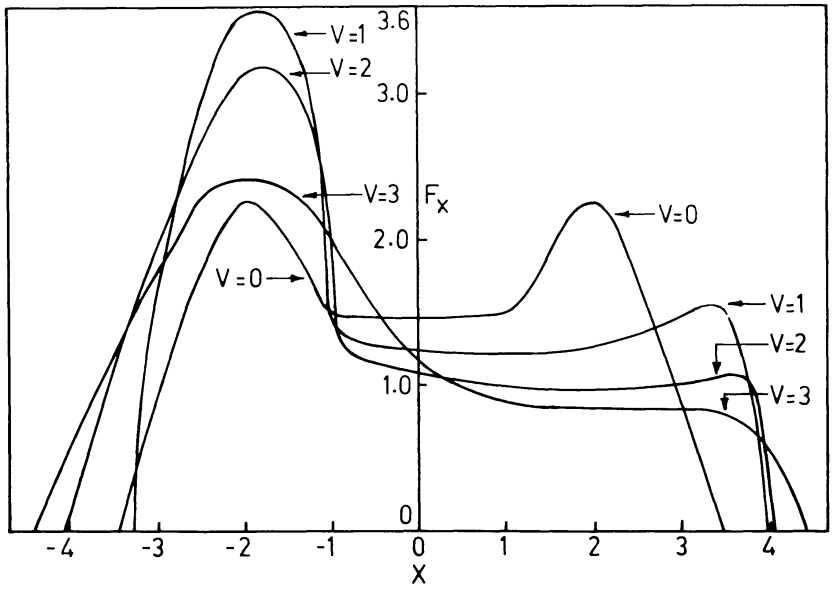

(b)

Fig. 5. Integrated profiles for R_I. $\varepsilon = 10^{-4}$, $\beta = 0$. (a) $B/A = 2$. (b) $B/A = 10$.

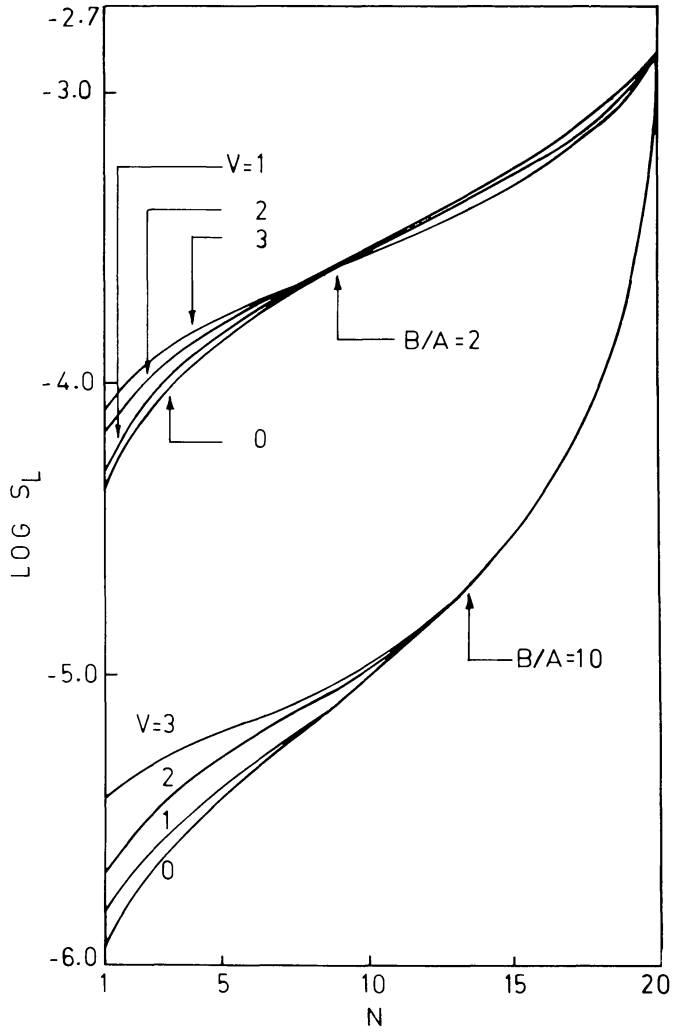

Fig. 6. Frequency independent source functions for R_I. $B/A = 2, 10$. $\varepsilon = \beta = 0$.

one on the blue side. We also notice a strong absorption in the core because of the fact that, unlike in the case of the medium, the emerging profiles of which are described in Figure 3, there is no continuous emission and the emission in the line contributes to the emission peaks shown here. When the gas is flowing radially outwards, the absorption is blue shifted and as the velocity increases this shift spreads into the blue side of the line and, therefore, we again observe an enhanced emission on the red side of the line and an almost flat portion on the blue side. When the geometrical extension is increased, the flatness on the blue side is quite apparent and also the line becomes broader for large velocities of the gas.

In Figure 6 the source functions for case (3) are plotted. This is a case of pure scattering and incident radiation has been given at the bottom of the atmosphere ($N = 20$) as there is no emission in the medium, which explains why the source functions are small at $N = 1$ and increase gradually towards $N = 20$.

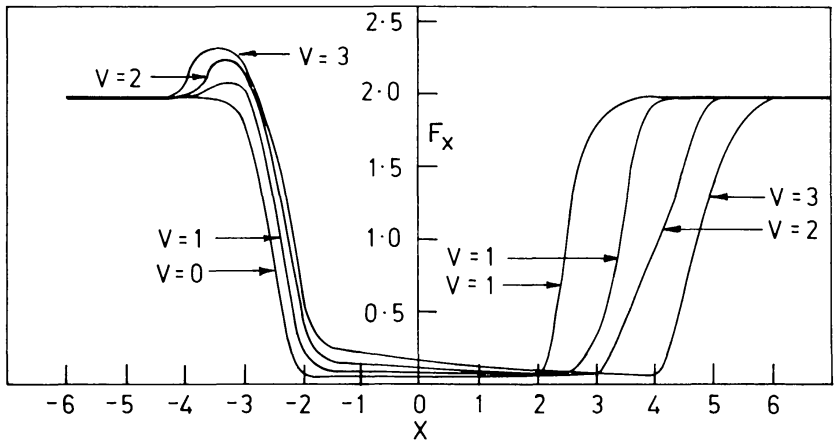

(a)

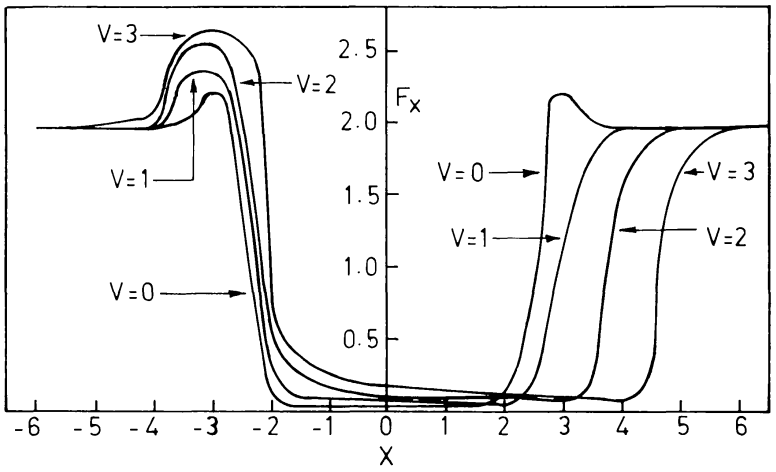

(b)

Fig. 7. Integrated profiles for R_I. $\varepsilon = \beta = 0$. (a) $B/A = 2$. (b) $B/A = 10$.

The integrated profiles corresponding to the source functions given in Figure 6 are presented in Figures 7a and 7b for $B/A = 2$ and 10, respectively. For static atmospheres, symmetric profiles emerge with no emission in the wings in the case of $B/A = 2$ and with a small amount in the more extended medium with $B/A = 10$. This is a purely geometrical effect. As there is no emission in either the continuum or in the line and scattering is the only means of transfer, we find an absorption line. However, as the velocity increases, a not too small emission in the wings on the red side of the line is found together with the shift of the centre of the line towards blue side and this emission increases with velocity and geometrical extension.

3. Conclusions

Lines in a differentially moving atmosphere have been calculated by using the angle averaged redistribution function R_I. These lines can be compared with those observed

for the gas velocities up to 3 thermal units. The lines formed in a purely scattering medium differ substantially from those formed in a medium where there is continuum and/or line emission exist.

References

Abhyankar, K. D.: 1964, *Astrophys. J.* **140**, 1353.

Bappu, M. K. V.: 1973, 'Wolf-Rayet and High Temperature Stars', in M. K. V. Bappu and J. Sahade (eds), *IAU Symposium*, No. 49, p. 59, D. Reidel Publishing Company.

Cannon, C. J. and Vardavas, I. M.: 1974, *Astron. Astrophys.* **32**, 85.

Chandrasekhar, S.: 1945, *Astrophys. J.* **102**, 402.

Hummer, D. G.: 1962, *Monthly Notices Roy. Astron. Soc.* **125**, 21.

Jefferies, J. T.: 1968, *Spectral Line Formation*, Blaisdell Publishing Company.

Kuhi, L. V.: 1973, 'Wolf-Rayet and High-Temperature Stars', in M. K. V. Bappu and J. Sahade (eds), *IAU Symposium* No. 49, p. 205, D. Reidel Publishing Company.

Kunasz, P. B. and Hummer, D. G.: 1974, *Monthly Notices Roy. Astron. Soc.* **166**, 57.

McCrea, W. and Mitra, K.: 1936, *Z, Astrophys.* **11**, 359.

Mihalas, D.: 1978, *Stellar Atmospheres*, Second Edition, Freeman Publishing Company.

Mihalas, D., Kunasz, P. B., and Hummer, D. G.: 1976, *Astrophys. J.* **210**, 250.

Peraiah, A.: 1978a, *Astrophys. Space Sci.* **58**, 189.

Peraiah, A.: 1978b, *Kodaikanal Obs. Bull.* **2**, 115.

Peraiah, A. and Wehrse, R : 1978, *Astron. Astrophys.* **70**, 213.

Vardavas, I. M.: 1974, *J. Quant. Spectr. Radiative Transfer* **14**, 909.

Vardavas, I. M.: 1976, *J. Quant. Spectr. Radiative Transfer* **16**, 781.

Wehrse, R. and Peraiah, A.: 1979, *Astron. Astrophys.* **71**, 289.